Journal of Medicinal Chemistry

Article

Synthesis and Mechanism of Action Studies of a Series of Norindenoisoquinoline Topoisomerase I Poisons Reveal an Inhibitor with a Flipped Orientation in the Ternary DNA–Enzyme–Inhibitor Complex As Determined by X-ray Crystallographic Analysis

Alexandra Ioanoviciu, Smitha Antony, Yves Pommier, Bart L. Staker, Lance Stewart, and Mark Cushman

J. Med. Chem., **2005**, 48 (15), 4803-4814• DOI: 10.1021/jm050076b • Publication Date (Web): 23 June 2005

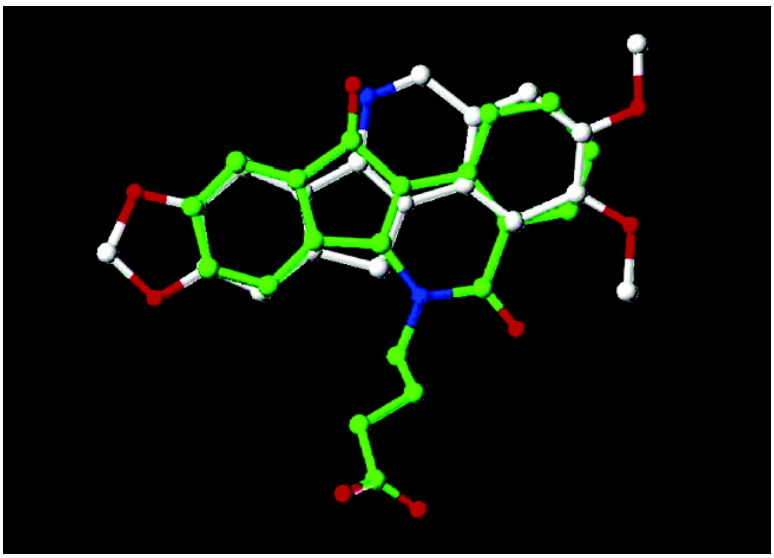

More About This Article

Additional resources and features associated with this article are available within the HTML version:

- Supporting Information
- Links to the 7 articles that cite this article, as of the time of this article download
- Access to high resolution figures
- Links to articles and content related to this article
- Copyright permission to reproduce figures and/or text from this article

View the Full Text HTML

Journal of Medicinal Chemistry is published by the American Chemical Society. 1155 Sixteenth Street N.W., Washington, DC 20036

Synthesis and Mechanism of Action Studies of a Series of Norindenoisoquinoline Topoisomerase I Poisons Reveal an Inhibitor with a Flipped Orientation in the Ternary DNA−Enzyme−Inhibitor Complex As Determined by X-ray Crystallographic Analysis

Alexandra Ioanoviciu,[†] Smitha Antony,[‡] Yves Pommier,[‡] Bart L. Staker,[§] Lance Stewart,[§] and Mark Cushman*[,†]

Department of Medicinal Chemistry and Molecular Pharmacology and the Purdue Cancer Center, School of Pharmacy and Pharmaceutical Sciences, Purdue University, West Lafayette, Indiana 47907, Laboratory of Molecular Pharmacology, Center for Cancer Research, National Cancer Institute, National Institutes of Health, Bethesda, Maryland 20892-4255, and deCODE biostructures, Inc., 7869 Northeast Day Road West, Bainbridge Island, Washington 98110

Received January 27, 2005

Several norindenoisoquinolines substituted with methoxy or methylenedioxy groups have been prepared and their anticancer properties evaluated in cancer cell cultures and in topoisomerase I inhibition assays. 2,3-Dimethoxy-8,9-methylenedioxy-11*H*-indeno[1,2-*c*]isoquinoline hydrochloride (**14**) is a strong topoisomerase I inhibitor and also displays very high cytotoxicity in the NCI cancer cell culture screen (mean graph midpoint of 50 nM). The X-ray crystal structure of norindenoisoquinoline **14** in complex with topoisomerase I and DNA has been solved, providing insight into the structure−activity relationships within this class of new anticancer agents. The number and position of the norindenoisoquinoline substituents have a significant influence on biological activity and demonstrate that substitution on the nitrogen atom is not an absolute requirement for the antitumor effect of the indenoisoquinolines. Removal of the 11-keto group from the lead compound **1** and replacement of the *N*-alkyllactam with an unsubstituted pyridine ring causes the indenoisoquinoline ring system to flip over in the DNA−enzyme−inhibitor ternary complex. This allows the nitrogen atom to assume the hydrogen bond acceptor role of the 11-keto group, resulting in hydrogen bonding to Arg364.

Introduction

The prospect of using indenoisoquinolines in cancer therapy arose as a result of the observation that the cytotoxicity profile of the indenoisoquinoline **1** (NSC 314622) is similar to the topoisomerase I (top1) inhibitor camptothecin (**2**), as indicated by a COMPARE analysis.[1] This originally suggested that compound **1** might be a topoisomerase I inhibitor, and in fact subsequent studies demonstrated that it inhibits the topoisomerase I-catalyzed DNA religation reaction in the DNA−enzyme−**1** ternary complex, and it displays moderate in vitro antiproliferative activity in cancer cells.[1] Topoisomerase I inhibitors such as camptothecin **(2)** and the indenoisoquinoline **1** that inhibit the DNA religation reaction are classified as topoisomerase "poisons", as opposed to "suppressors", which inhibit the enzyme-catalyzed DNA cleavage reaction. Interest in the potential clinical applications of indenoisoquinolines stems from the fact that compounds from this class possess the desired topoisomerase I inhibitory activity and cancer cell cytotoxicity of camptothecin but potentially lack some of the disadvantages inherent in camptothecin therapy. Although camptothecin is cytotoxic in a wide range of animal tumors, its duration of action is limited due to rapid reversibility of the ternary DNA−enzyme−camptothecin complex and hydrolysis of the lactone to a hydroxyacid that binds to plasma proteins.[2,3] Moreover, some cancer cells develop resistance to camptothecin. In this context, there is a need for chemically stable compounds that act as topoisomerase I inhibitors and possess cytotoxicity in cancer cell lines.

5,11-Diketoindenoisoquinoline analogues of **1** bearing various substituents on the nitrogen atom have been previously synthesized and tested for biological activity.[1,4] Also, indenoisoquinolinium salts such as **3** have been shown to inhibit topoisomerase I and display cytotoxicity against cancer cells in the in vitro NCI screen and in the hollow fiber animal model.[5,6] A variety of indenoisoquinolines related to **1** and **3** display different DNA cleavage site specificities relative to camptothecin, raising the prospect that different types of cancers could be targeted to provide an antitumor spectrum complementary to the existing therapeutic agents.[7,8]

All of the previously studied indenoisoquinolines have had a substituent on the nitrogen. Herein we evaluate for the first time the antitumor properties of norindenoisoquinolines, which lack a substituent on the nitrogen atom. The present study aimed to define the role of different aromatic ring substitution patterns and to assess the role of N-6 substitution in the anticancer properties and topoisomerase I inhibitory activity of these compounds. Moreover, the indenoisoquinolines in the present series lack a hydrogen bond-accepting C-11 carbonyl group, which bonds to the Arg364 side chain of the enzyme.[9] Another goal of the present investigation was to determine whether this group could be deleted

* To whom correspondence should be addressed: Tel: 765-494-1465. Fax: 765-494-6790. E-mail: cushman@pharmacy.purdue.edu.
[†] Purdue University.
[‡] NIH, Bethesda, MD.
[§] deCODE biostructures.

10.1021/jm050076b CCC: $30.25
Published on Web 06/23/2005

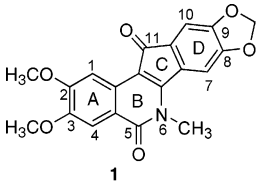

1
NSC 314622

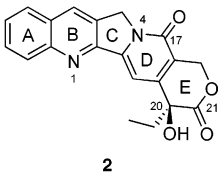

2
camptothecin

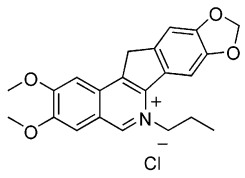

3

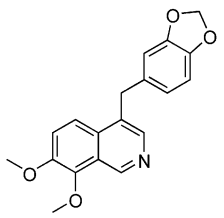

4

in the norindenoisoquinoline series with retention of activity. To pursue these aims, it was also necessary to explore the scope and regiochemistry of a modified Pomeranz−Fritsch strategy for the synthesis of norindenoisoquinolines.

Results and Discussion

Chemistry. In the literature there are isolated reports of norindenoisoquinoline syntheses in low yields. Compounds **13** and **14** have been prepared by the route shown in Scheme 1.[10,11]

The approach investigated here leads to double-cyclization products resulting from a bimolecular reaction. The first cyclization takes place in an intramolecular fashion and involves the aminoacetal (Scheme 1). Then a bimolecular reaction with a benzaldehyde derivative occurs followed by a second critical cyclization. Compounds such as **4**, which do not require a second cyclization, have been prepared successfully using the Bobbitt conditions.[11−13] These arise from the bimolecular reaction of the aminoacetal-derived intermediates with benzaldehydes.

There are numerous reports of intramolecular cyclizations of aminoacetals.[14] Aminoacetals or acetals have been widely used to build heterocycles as well as carbocycles, and there are examples of successful double intramolecular cyclizations leading to compounds such as **5** or **6**.[15,16]

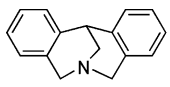

5

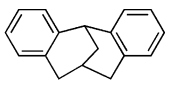

6

The Pomeranz−Fritsch reaction[17] and its newer versions[18,19] are generally favored by electron-donating substituents. The traditional Pomeranz−Fritsch approach is known to provide low yields of products and subsequent modifications of the reaction have been intended to address this difficulty. For example, to improve the use of aminoacetals in the Pomeranz−Fritsch-type reactions, a variety of acids have been employed such as triflic, perchloric,[15,16] polyphosphoric,[20] trifluoroacetic, methanesulfonic, hydrochloric/acetic, sulfuric,[21] and hydrochloric acids.[18] The reactions for simple isoquinolines have been demonstrated to proceed at lower temperatures as well.[15,16] On the other hand, when aminoacetals were used as starting materials for compounds such as the **4**, which result from an intramolecular cyclization followed by a bimolecular reaction with a benzaldehyde, the bimolecular reactions were favored by higher temperatures.[12]

In the present case, harsh conditions were used. Boiling concentrated hydrochloric acid or trifluoroacetic acid afforded the oxygenated norindenoisoquinolines, which were prepared as depicted in Schemes 1−5. Briefly, the general approach involves the condensation of aminoacetaldehyde dimethyl acetal with a benzalde-

Scheme 1[a]

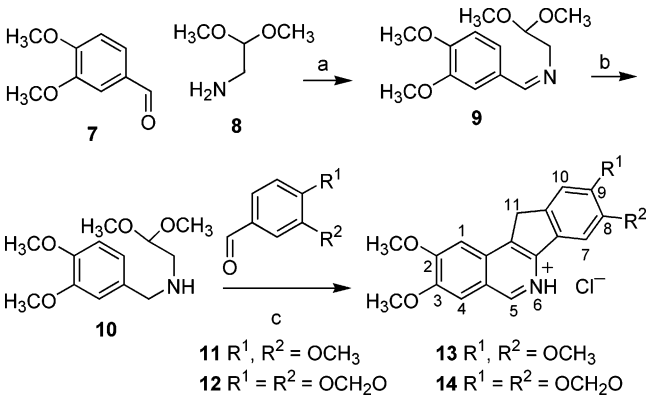

11 R^1, R^2 = OCH_3 **13** R^1, R^2 = OCH_3
12 $R^1 = R^2 = OCH_2O$ **14** $R^1 = R^2 = OCH_2O$

[a] Reagents: (a) benzene/Δ; (b) $NaBH_4$, CH_3CH_2OH; (c) HCl.

Scheme 2[a]

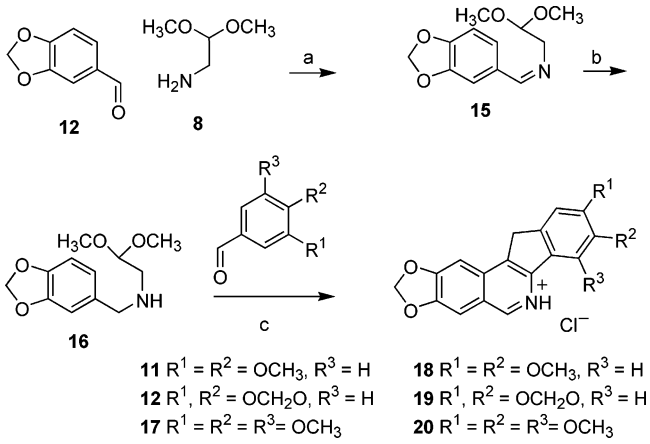

11 $R^1 = R^2 = OCH_3$, R^3 = H **18** $R^1 = R^2 = OCH_3$, R^3 = H
12 R^1, $R^2 = OCH_2O$, R^3 = H **19** R^1, $R^2 = OCH_2O$, R^3 = H
17 $R^1 = R^2 = R^3 = OCH_3$ **20** $R^1 = R^2 = R^3 = OCH_3$

[a] Reagents: (a) benzene/Δ; (b) $NaBH_4$, CH_3CH_2OH; (c) HCl or TFA.

Scheme 3[a]

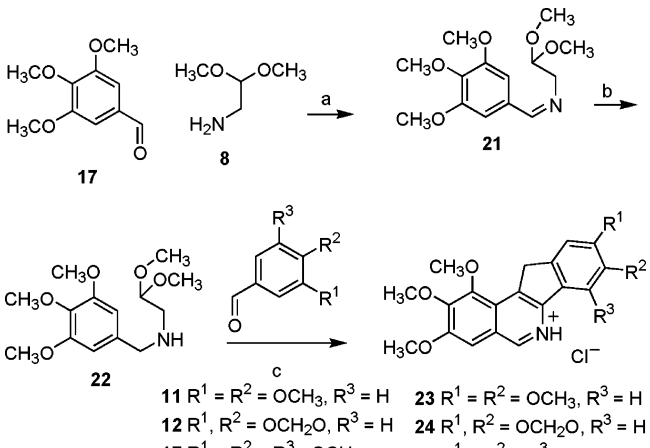

11 $R^1 = R^2 = OCH_3$, R^3 = H **23** $R^1 = R^2 = OCH_3$, R^3 = H
12 R^1, $R^2 = OCH_2O$, R^3 = H **24** R^1, $R^2 = OCH_2O$, R^3 = H
17 $R^1 = R^2 = R^3 = OCH_3$ **25** $R^1 = R^2 = R^3 = OCH_3$

[a] Reagents: (a) $CHCl_3$, $MgSO_4$; (b) $NaBH_4$, CH_3CH_2OH; (c) HCl.

Scheme 4[a]

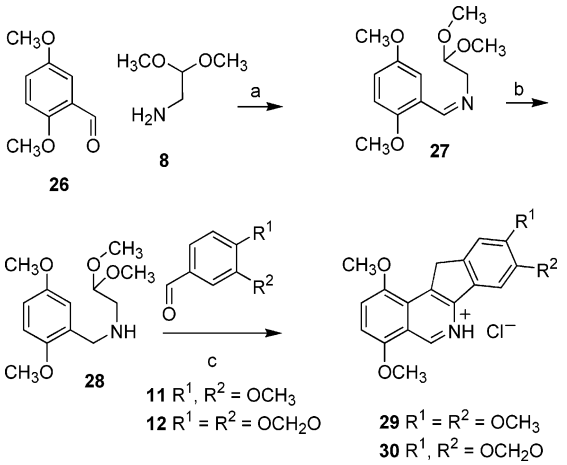

[a] Reagents: (a) $CHCl_3$, $MgSO_4$; (b) $NaBH_4$, CH_3CH_2OH; (c) HCl.

Scheme 5[a]

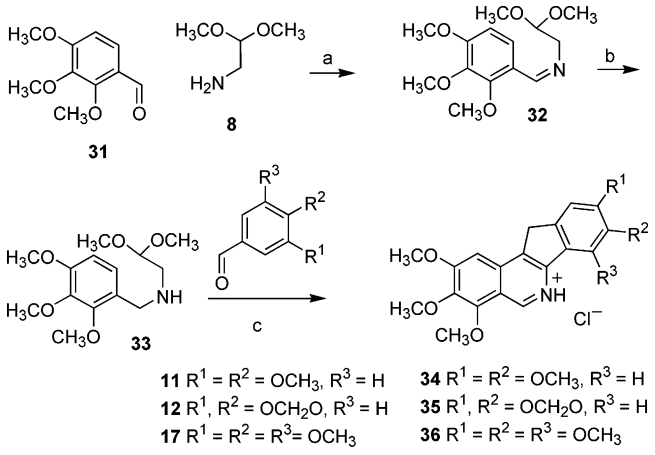

[a] Reagents: (a) benzene/Δ; (b) $NaBH_4$, CH_3CH_2OH; (c) HCl.

hyde derivative to afford the corresponding imine. Reduction of the Schiff base was found to proceed best using sodium borohydride in ethanol at reflux. The secondary amine obtained in this step was reacted with a substituted benzaldehyde in a strongly acidic environment, either concentrated hydrochloric acid or trifluoroacetic acid at 100 °C, conditions that led to the formation of tars. The target compounds were then isolated as hygroscopic hydrochloride salts. In all cases, only one of the theoretically possible regioisomers was isolated, and the structures of the products were readily apparent from the appearance of the aromatic protons as singlets in the ^{1}H NMR spectra.

Compounds **13** and **14** have been synthesized previously using the route outlined in Scheme 1.[10] However, their antitumor effects had not been investigated before. The remaining norindenoisoquinolines are novel compounds. The present investigation demonstrates that this synthetic approach is versatile and can be extended to obtain a wide variety of analogues possessing oxygenated substituents. This route provides rapid access to the synthetic targets and requires the use of starting materials that are either commercially available or can be obtained quantitatively from commercially available substances. The overall yields for the synthesis of norindenoisoquinolines are determined by the last step, which is a modification of the Pomeranz–Fritsch isoquinoline synthesis.[17] The method provides a relatively direct means of building the norindenoisoquinoline system when electron-donating groups such as a methylenedioxy bridge or methoxy substituents are present on both aromatic rings. It is also complementary to other methods of indenoisoquinoline synthesis.[4,22]

Scheme 6

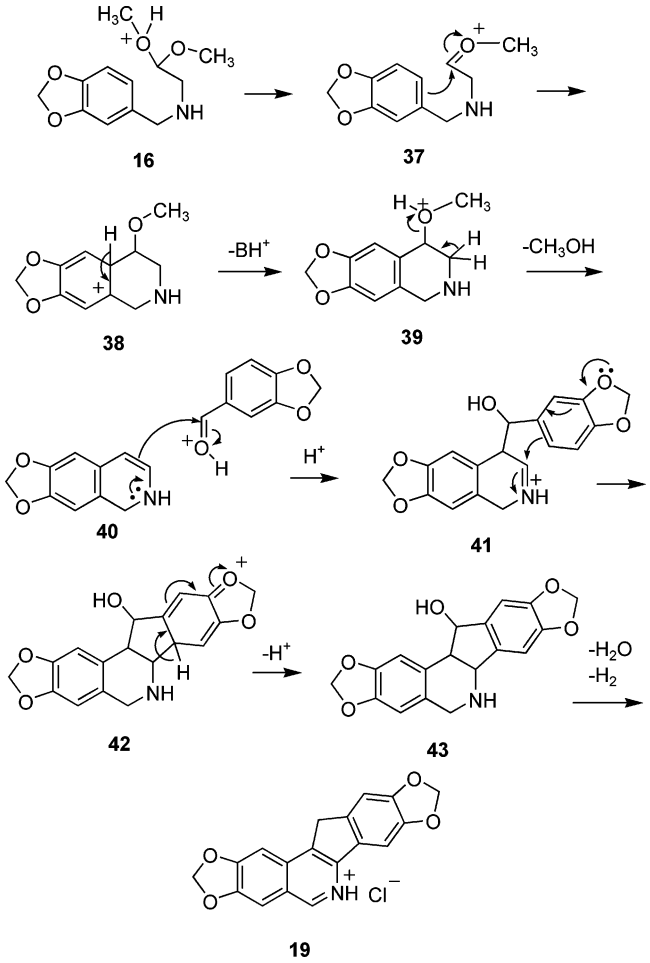

Reaction Mechanism. The proposed mechanism for the key reaction is depicted in Scheme 6. The first cyclization begins with the elimination of methanol from the protonated intermediate **16**, followed by the attack of the aromatic ring on the resulting cation **37**. This first step is the same as in the Pomeranz–Fritsch isoquinoline synthesis as well as in its improved versions such as the Bobbitt[13] or Jackson modifications.[19] In the traditional Pomeranz–Fritsch synthesis the presence of the protonated imine group results in partial deactivation of the phenyl ring,[17] an effect that was overcome in the later versions such as in the Bobbitt reaction by using the corresponding amine, which is more stable to hydrolysis. The formation of the first ring is favored by electron-donating substituents para or ortho to the position of ring closure.[23]

As already mentioned, methoxy groups are strongly activating in this process. As reported previously,[13,24–27] we find that both methylenedioxy or methoxy groups cause ring closure to occur preferentially in the para position as opposed to ortho. In all cases, during the first cyclization, when two products are possible, only the para cyclized isomer was isolated. Thus compounds **13**, **14**, **18**, **19**, and **20** formed.

Table 1. Cytotoxicities and Topoisomerase I Inhibitory Activities of Indenoisoquinoline Analogues

	cytotoxicity (GI_{50} in μM)[a]									
compd	lung HOP-62	colon HCT-116	CNS SF-539	melanoma UACC-62	ovarian OVCAR-3	renal SN12C	prostate DU-145	breast MDA-MB-435	MGM[b]	Top 1 cleavage[c]
1	1.30	35	41	4.2	73	68	37	96	20.0	++
2	0.01	0.03	0.01	0.01	0.22	0.02	0.01	0.04	0.0405	++++
14	0.0721	>100	<0.01	<0.01	NT[d]	>100	0.0281	<0.01	0.0505	+++
13	NT[d]	>50	>50	>50	>50	>50	>50	>50	44.7	++
18	NT[d]	11.1	23.4	>100	61.2	>100	25.3	63.4	33.9	+++
19	0.227	0.283	0.598	0.190	0.0232	0.0414	NT[d]	<0.01	0.272	++
20	21.7	18.8	NT[d]	19.3	15.5	13.4	23.2	13.2	20.9	0
23	34.8	31.8	14.0	7.42	15.9	14.4	21.7	16.2	19.1	+
24	0.234	0.0694	0.869	0.439	0.403	0.602	>100	0.178	2.01	++
25	35.4	33.5	NT[d]	17.4	19.1	17.6	26.6	20.8	24	0
29	21.4	17.8	14.0	18.0	15.4	14.8	28.1	23.4	18.6	0
30	<0.01	0.249	NT[d]	>100	26.9	>100	48.4	>100	24.5	++
34	16.0	8.81	NT[d]	3.84	0.529	NT[d]	NT[d]	NT[d]	13.2	++
35	NT[d]	22.1	NT[d]	22.4	NT[d]	NT[d]	26.9	>100	26.3	++
36	28.5	27.8	NT[d]	21.1	21.5	20.3	29.6	23.0	26.3	++

[a] The cytotoxicity GI_{50} values are the concentrations corresponding to 50% growth inhibition. [b] Mean graph midpoint for growth inhibition of all human cancer cell lines successfully tested. [c] The compounds were tested at concentrations ranging up to 10 μM. The activity of the compounds to produce top 1-mediated DNA cleavage was expressed semiquantitatively as follows: 0: no activity; +: weak activity; ++: similar activity as the parent compound **2**; +++ and ++++: greater activity than the parent compound **2**; ++++: similar activity as 1 μM camptothecin. [d] NT = not tested.

The rearomatization of the phenyl ring then leads to intermediate **39**. Although intermediate **39** is shown as a 4-methoxy-1,2,3,4-tetrahydroisoquinoline, it is likely that the corresponding 4-hydroxy tetrahydroisoquinoline is present as well. Such hydroxyl derivatives are unstable products that have been isolated before when the reaction was run at low (room) temperature.[28] Loss of methanol from intermediate **39** results in the formation of the 1,2-dihydroisoquinoline **40**, an unstable compound that is considered to be an intermediate in the modified Pomeranz–Fritsch reactions.[12,13,19] The first cyclization does not depend on the presence of the nitrogen atom in the 2 position. Precedents exist when the nitrogen atom was either acylated,[21] tosylated (the Jackson modification),[19] or altogether absent from the molecule,[16] and yet the first step proceeded successfully for phenyl rings activated by electron-donating substituents.

It is in the next step leading to intermediate **41** that the presence of the nitrogen is essential. The lone electron pair on the nitrogen atom facilitates the nucleophilic attack on the protonated benzaldehyde derivative. The protonation of the substituted benzaldehyde also further deactivates the aromatic ring and prevents its attack by electrophiles, thus minimizing competing reactions at this stage.

Subsequent attack of the iminium ion **41** by the second aromatic ring leads to the formation of the second ring, as previously hypothesized.[29] Due to their electrophilic character, iminium ions similar to **41** were considered to be intermediates in other reactions.[30] It can be inferred that activation of the second aromatic ring from the substituted benzaldehyde is important, and the present results demonstrate that methoxy and methylenedioxy groups have a para-directing effect. Again, whenever there is a choice between ortho or para ring closure, the second cyclization affords para-cyclized products, namely **13**, **14**, **18**, **19**, **23**, **24**, **22**, **29**, **30**, **34**, and **35**. The rearomatization of **42** to **43** is then followed by dehydration and dehydrogenation to afford the final norindenoisoquinoline.

A secondary mechanism that may also be involved is shown in Scheme 7. Intermediate **41** may isomerize to

Scheme 7

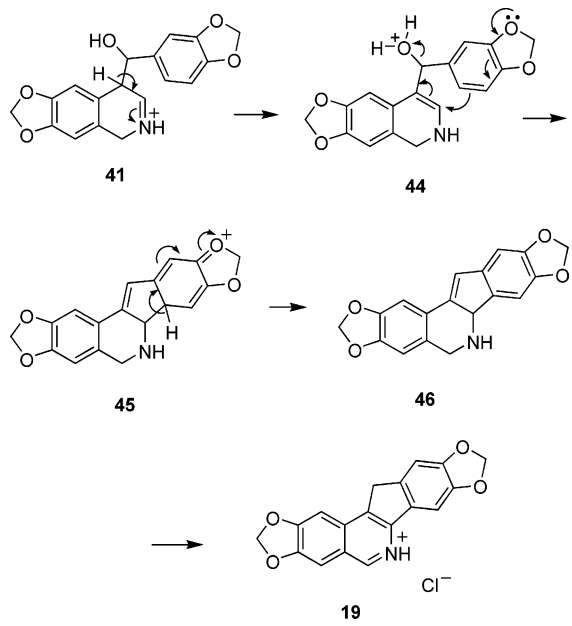

44 and the second cyclization could occur then as the benzylic hydroxyl is lost in the acidic medium[10] to form intermediate **45**, which can be rearomatized to **46** and dehydrogenated to the norindenoisoquinoline **19**.[10]

Biological Results. All norindenoisoquinolines were tested at the National Cancer Institute for their ability to inhibit the proliferation of approximately 55 human cancer cell lines. The GI_{50} values for several selected cell lines and the mean graph midpoints (MGM) are presented in Table 1. The MGM is based on a calculation of the average GI_{50} for all of the cell lines tested (approximately 55) in which GI_{50} values below and above the test range (10^{-8} to 10^{-4} molar) are taken as the minimum (10^{-8} molar) and maximum (10^{-4} molar) drug concentrations used in the screening test. Therefore, the MGM value represents an overall assessment of toxicity of the compound across numerous cell lines. The results of topoisomerase I DNA cleavage experiments are expressed semiquantitatively and provide a means of comparison with the biological activity of

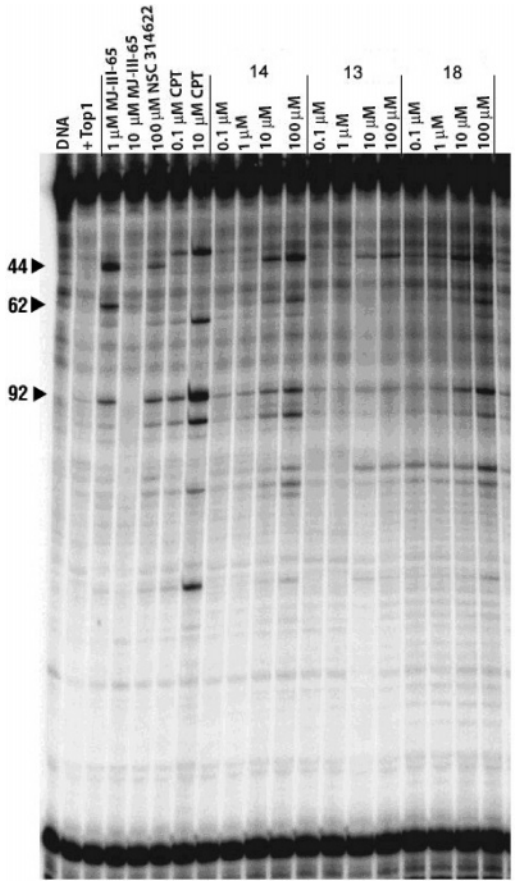

Figure 1. Comparison of the topoisomerase I-mediated DNA cleavage products of pBluescript SK(−) phagemid DNA at various drug concentrations as indicated. The assays were carried out at room temperature for 30 min and stopped by adding 0.5% SDS. The resulting DNA fragments were separated using 16% denaturing polyacrylamide gel electrophoresis. Topoisomerase I was present in all reaction mixtures except for the one corresponding to the first lane.

camptothecin **(2)** (++++) and with the parent compound **1** (++).

The cytotoxicities of most of the compounds were in the micromolar range. Compound **14** was quite active with an average MGM of 50 nM. The norindenoisoquinoline **14** is also a good topoisomerase I inhibitor (+++). Interestingly, compound **18**, in which the locations of the di(methoxy) and methylenedioxy substituents are exchanged relative to **14**, inhibits topoisomerase I to the same extent as norindenoisoquinoline **14** (Figure 1). However, the cytotoxicity of **18** (33.9 μM) is much lower than that of **14**. This suggests either that compound **18** does not reach its biological target as efficiently as **14** in intact cells, or that compound **14** may have an alternate cellular target. Differences in metabolism could also possibly explain the observed results.

Replacement of the methylenedioxy substituent in positions 8 and 9 of **14** with two methoxy groups drastically reduced biological activity. Compound **13** has a low cytotoxicity (44.7 μM) and it inhibits topoisomerase I moderately (++).

Compound **19** displays submicromolar cytotoxicity, yet it appears to be only a moderately active topoisomerase I poison. Most of the remaining norindenoisoquinolines had moderate cytotoxicities ranging from

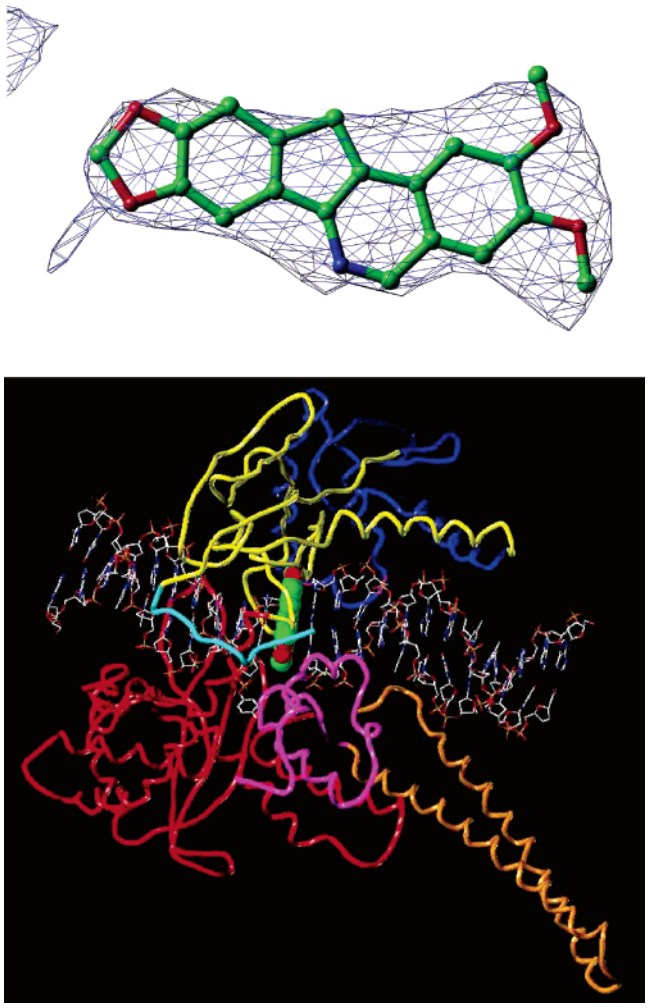

Figure 2. Top: Electron density ($|F_o| - |F_c|$ at 3.1 Å, contoured at 2σ) showing the initial unbiased experimental density used for the placement of compound **14** into the topo70−DNA covalent complex crystal structure. Bottom: Diagram of the topo70−DNA complex bound with indenoisoquinoline **14**. The topoisomerase I inhibitor **14** is displayed as a space-filling model (CPK). The N-terminal fragment is colored in cyan, the core subdomain I yellow, subdomain II blue, subdomain III red, the linker is orange and the C-terminus is magenta. The oligonucleotide is represented as capped sticks and is colored according to atom type.

13.2 μM to 26.3 μM, with the exception of compound **24**, which had an MGM in the low micromolar range (2.0 μM).

All of the compounds were examined for induction of DNA cleavage in the 3′-end-labeled *Pvu*II/*Hind*III fragment of pBluescript SK(−) phagemid DNA in the presence of top1.[1] The cleavage patterns for the norindenoisoquinolines **13**, **14**, and **18** are displayed in Figure 1, along with those of the lead indenoisoquinoline **1** (NSC 314622), indenoisoquinoline **49**[4,8] (MJ-III-65) with enhanced potency relative to **1**, and camptothecin (**2**, CPT). Some, but not all, of the DNA cleavage sites observed with the norindenoisoquinolines were different from each other, and there were also some differences relative to the indenoisoquinolines and camptothecin. For example, the camptothecin band at site 37 was not seen with the indenoisoquinolines or with the norindenoisoquinolines in Figure 1, and the band at site 44 was observed with the indenoisoquinolines and norinde-

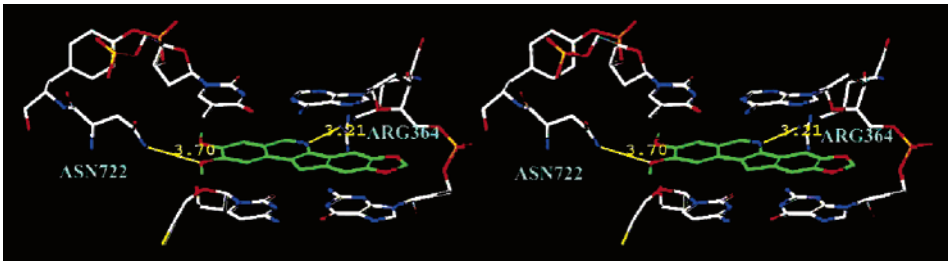

Figure 3. Crystal structure of norindenoisoquinoline **14** in complex with topoisomerase I and DNA.

noisoquinolines but not with camptothecin. Some differences are also apparent in comparison of the norindenoisoquinolines vs the indenoisoquinolines. These differences are important because they indicate that different cancer cell genes could be targeted more selectively with one type of inhibitor vs another. Also, similar to the situation with other anticancer drugs that share a single target (e.g. top2 and tubulin inhibitors), it can be expected that different top1 inhibitors will have different spectra of antitumor activity.[31] Similar conclusions have been reached in prior top1-DNA cleavage studies involving other indenoisoquinolines.[4−6,19,32]

Crystal Structure and Molecular Modeling. Norindenoisoquinoline **14**, as the biological assays indicate, is an efficient topoisomerase I poison. Its mechanism of action, involving inhibition of the DNA religation reaction in the ternary complex, is similar to that proposed for topotecan.[33] The crystal structure of the ternary cleavage complex involving **14** was determined and the resulting electron density omit map for the drug molecule **14** is shown in Figure 2 (top). The asymmetry of the electron density makes a clear argument for the correct placement of the indenoisoquinoline **14** in the ternary complex (Figure 2, bottom). As shown in Figure 3, the structure reveals that the norindenoisoquinoline inserts between the DNA base pairs in the ternary cleavage complex at the cleavage site. Stacking interactions as well as two direct hydrogen bonds to enzyme residues Arg364 and Asn722 then stabilize the ternary complex. These interactions may help to explain why norindenoisoquinoline **14** is a stronger topoisomerase I poison than **47**, which uses the oxygen atom from the

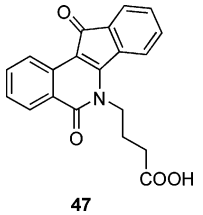

47

C11 carbonyl to hydrogen bond to residue Arg364, but lacks a second hydrogen bond to the protein.[9] The overlay of these two ligands in their respective ternary complex crystal structures (Figure 4) indicates that in fact the heterocyclic nitrogen atom of the norindenoisoquinoline **14** is placed in the same position as the C-11 oxygen atom of the ketone carbonyl group of **47**, so that **14** is flipped over relative to **47** in the cleavage complex. This positioning implies that the nitrogen atom of **14** is not protonated and is free to use its electon pair to stabilize the interaction with topoisomerase I. At neutral pH, norindenoisoquinoline **14** exists as the free base.

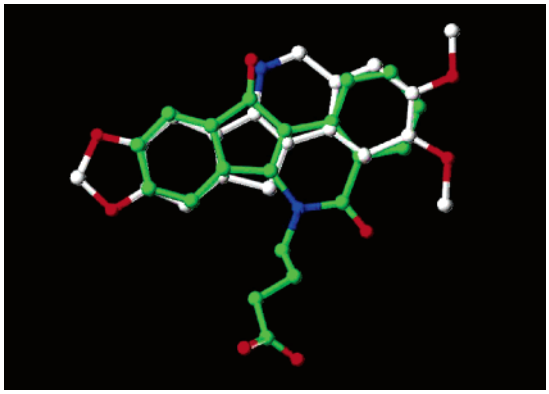

Figure 4. Overlay of the norindenoisoquinoline **14** (white carbon atoms) and the 5,11-diketoindenoisoquinoline **47** (green carbon atoms) in their ternary cleavage complexes as determined by X-ray crystallography.

The crystal structure of the camptothecin (**2**) ternary complex shows that Arg364 participates in hydrogen bonding to the N1 of camptothecin.[9] Camptothecin also forms two hydrogen bonds to topoisomerase I while intercalating between the DNA bases pairs.[9] The cytotoxicities of camptothecin and norindenoisoquinoline **14** are in the same range (40.5 nM vs 50 nM), although the topoisomerase I DNA cleavage assays suggest that norindenoisoquinoline **14** is a weaker topoisomerase I inhibitor than camptothecin.

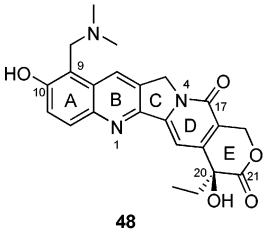

48
topotecan

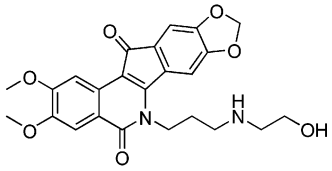

49 (MJ-III-65)

As compared to topotecan (**48**), norindenoisoquinoline **14** has a larger number of direct contacts with the topoisomerase I residues. Topotecan has only one direct hydrogen bond to the enzyme, between the C20 hydroxyl and the carboxylate oxygen of Asp533.[9] Residue Asp533 is in fact located in the immediate vicinity of Arg364, to which it hydrogen bonds. Therefore, both norindenoisoquinoline **14** and topotecan (**48**) have a point of attachment to the enzyme in the minor groove region of the DNA. The hydrolyzed, hydroxyacid form of topotecan also participates in water-mediated hydrogen bonding with residues Asn722 and Tyr723.

In the case of norindenoisoquinoline **14**, there is a direct interaction between one methoxy oxygen atom and the side chain amide nitrogen of Asn722, which is

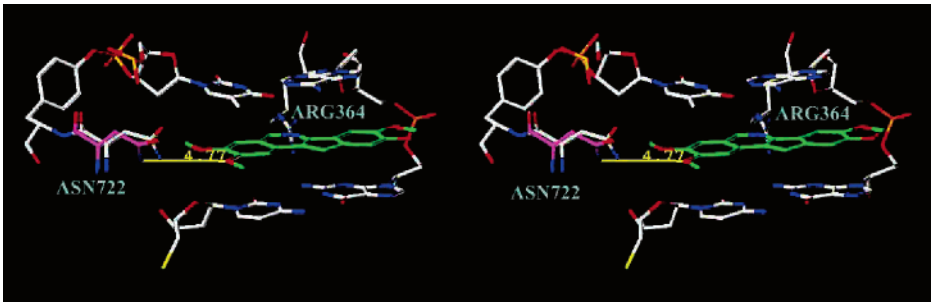

Figure 5. Overlay of Asn722 from the topotecan ternary complex (Asn722 carbon atoms magenta) with the norindenoisoquinoline **14** cleavage complex (Asn722 colored by atom type). The figure documents the movement of Asn722 toward **14** in its cleavage complex relative to the position of Asn722 in the topotecan complex. The indenoisoquinoline **14** is displayed in green. The figure is programmed for wall-eyed (relaxed) viewing.

placed in the region between the two methoxy substituents. The methyl groups are pointed away from Asn722, and this key feature allows the hydrogen bond to form. Figure 5 displays the region around the norindenoisoquinoline **14** in its crystal structure, and Asn722 from the topotecan complex structure is overlayed and shown in magenta. In the case of norindenoisoquinoline **14**, Asn722 moves toward the ligand and attains the correct conformation to participate in hydrogen bonding. It is also interesting that the carbon atoms of the two methoxy substituents on the norindenoisoquinoline lie in the same plane as the heterocycle. This is not in fact the lowest energy conformation for the isolated ligand. Most likely the methoxys become coplanar with the aromatic rings of the norindenoisoquinoline as a result of steric interactions with the DNA base pairs above and below. Computer modeling in Sybyl of the other norindenoisoquinolines has indicated that when the ligand is prepositioned in the binding site according to the information provided by the crystal structure, during energy minimization there is a tendency to bring methoxy substituents in the plane of the norindenoisoquinoline heterocycle whenever possible.

The crystal structure of norindenoisoquinoline **14** suggests that stacking interactions are crucial for efficient bonding to the covalent DNA topoisomerase I cleavage complex. The biological assays reveal that the larger substituents around the indenoisoquinoline nucleus are not well tolerated and result in decreased biological activity. The methoxy groups in the structures of most norindenoisoquinoline have the potential to act as hydrogen bond acceptors. A larger number of bulky substituents, however, especially the presence of three adjacent methoxy groups, is difficult to accommodate in the cleavage complex. As the van der Waals surface of the energy minimized inactive compound **25** in Figure 6 indicates, repulsive interactions among the three substituents on the same phenyl ring result in some being placed above the plane of the heterocycle while some are located below. The steric clashes among the adjacent methoxy groups confer increased bulk to the molecule, which in turn is expected to disrupt stacking with the DNA base pairs in the cleavage complex and is likely the cause of its poor activity.

Steric bulk in the ligand is especially poorly tolerated in the vicinity of the nonscissile phosphodiester bonds. Replacement of the methylenedioxy bridge in **14** with two methoxy groups in compound **13** leads to diminished biological activity, most likely due to unfavorable van der Waals contacts between the additional methoxy and

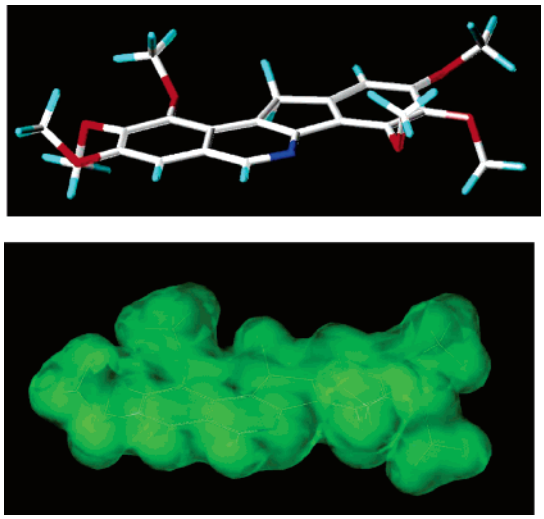

Figure 6. Top: norindenoisoquinoline **25** is displayed according to atom types in a capped sticks model. Bottom: the translucent van der Waals surface of norindenoisoquinoline **25** is displayed in green.

the phosphodiester backbone. Comparison of the crystal structures of ternary complexes derived from a variety of topoisomerase I inhibitors has indicated a very snug fit on the side of the binding pocket next to the nonscissile DNA strand.[9] This fact is consistent with the inactivity of the more bulky trimethoxylated compounds **20** and **25** as topoisomerase I inhibitors.

Last, a methoxy substituent in position 7 has a shielding effect on the nitrogen atom and interferes with the hydrogen bond formation between the isoquinoline heterocyclic nitrogen and Arg364. The methoxy substituent could be considered as a hydrogen bond acceptor, yet it is itself prevented from forming a hydrogen bond to Arg364 due to repulsive van der Waals interactions, which are calculated to orient it with the methyl protruding toward the arginine ϵ-nitrogen. The resulting effect of the six methoxy substituents in the case of compound **25** is that during energy minimization the ligand is moved away from Arg364 by about 1 Å. Interference of the 7-methoxy group with hydrogen bonding to Arg364 may also contribute to the inactivity of **20** as a topoisomerase I inhibitor.

Norindenoisoquinoline **19** constitutes a particular case, since it is the least voluminous of all of the compounds reported here. Although it is quite cytotoxic, it is a moderately potent inhibitor of topoisomerase I.

Figure 7 depicts the electrostatic potential surfaces of indenoisoquinolines **1**, **3** and **14** calculated using

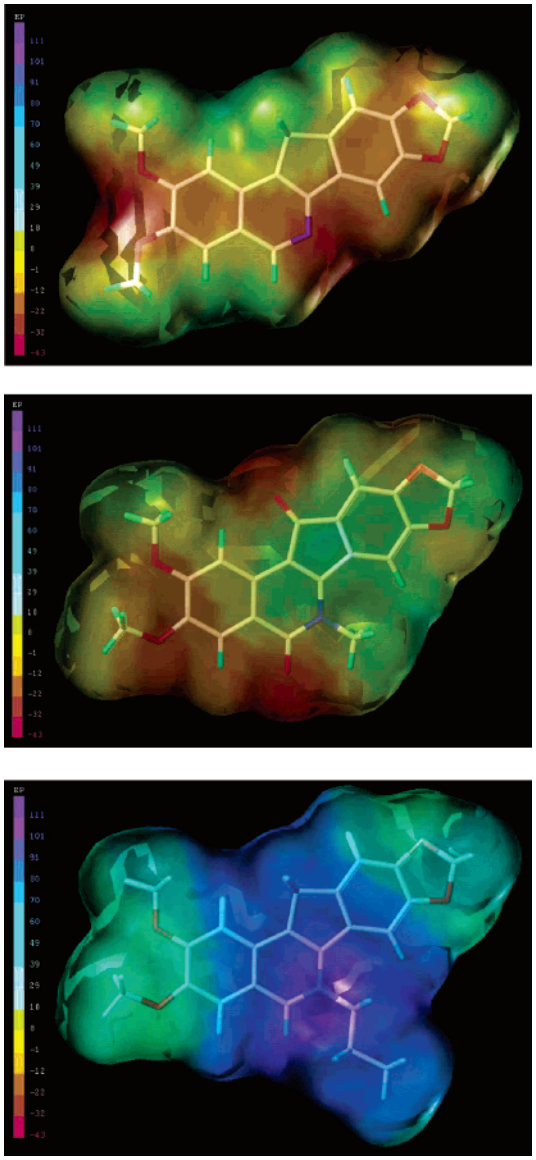

Figure 7. Electrostatic potential surfaces for **14** (top), **1** (middle), and **3** (lower) calculated using MMFF94 charges.

MMFF94 charges. Red contours correspond to regions that are relatively electron-rich, whereas blue areas indicate relatively electron-poor regions within each molecule. There are obvious differences in the electron distributions of these three compounds in the regions containing the nitrogen atom and the C-11 carbon atom. As compared to the indenoisoquinolinium salts, the nitrogen atom in the norindenoisoquinolines is not expected to be charged at physiological pH. A neutral norindenoisoquinoline uses the nonprotonated nitrogen as a hydrogen bond acceptor from Arg364. The electron density on the nitrogen atom in the case of norindenoisoquinolines is higher than in the 5,11-diketoindenoisoquinolines, like **1**, where the nitrogen is part of a lactam moiety. Also the nitrogen atom, being unsubstituted in norindenoisoquinolines, is not sterically hindered from participating in bonding interactions with biological macromolecules, resulting in the "flipped" orientation of **14** in the cleavage complex relative to **47** (Figure 4).[9] It is clear from Figure 7 (top) that the region of high electron density in **14** corresponds to the nitrogen, while in the lead compound **1** (middle) it is the 11-ketone oxygen. These features allow norindenoisoquinolines to interact differently with topoisomerase I than 5,11-diketoindenoisoquinolines such as **1** and **47**. For this reason, the structure−activity relationships derived for this series are not expected to correlate exactly with the other subclasses of indenoisoquinolines.

Conclusion

The modified Pomeranz−Fritsch strategy is generally applicable to the synthesis of norindenoisoquinolines and affords the desired products in yields ranging from 5% to 52%. The methoxy or methylenedioxy groups display a para-directing effect in both cyclizations involved in the formation of the indenoisoquinoline system. Only para-substituted products were isolated whenever both ortho and para positions to the activating substituent were free. This method allows the rapid assembly of norindenoisoquinolines that would be difficult to synthesize otherwise.

Structural requirements for antitumor properties in the norindenoisoquinoline series are very strict. Substitution with two methoxy groups in positions 2 and 3 and a methylenedioxy bridge in positions 8 and 9 confers the highest anticancer activity. Compound **14** is in fact more cytotoxic than the alkyl-substituted indenoisoquinolium salts[5,6] and it also compares favorably with many compounds in the 5,11-diketoindenoisoquinoline series.[1,4,5] From this evidence, it can be concluded that a substituent on the nitrogen atom is not essential for biological activity. However, the presence of such a substituent atom is likely to alter the binding mode of the molecule to its cellular targets. It is also apparent that the 11-keto group is not essential for maximum activity, since the nitrogen atom in the norindenoisoquinolines can play the role of the 11-keto oxygen atom of the 5,11-diketo-*N*-alkylindenoisoquinolines when bound in the ternary cleavage complex. This fact is demonstrated in the "flipped over" orientations of the two systems in the cleavage complex as shown in Figure 4. The inactivities of the trimethoxylated indenoisoquinolines **20** and **25** as topoisomerase I inhibitors can be explained as the result of (1) steric interference with the requirement for planarity in the intercalation site; (2) lack of sufficient space next to the nonscissile DNA strand to accommodate increased steric bulk, and (3) interference of the C-7 methoxy group with hydrogen bonding between the 11-ketone and the side chain of Arg364.

Experimental Section

Melting points were determined in capillary tubes and are uncorrected. Except where noted, ^{1}H NMR spectra were obtained using $CDCl_3$ as solvent and the solvent peak as internal standard. ^{1}H NMR spectra were determined at 300 MHz. Electrospray mass spectra were obtained using a FinniganMATT LCQ (Thermoquest Corp., San Jose, CA) instrument at the Purdue Campus-Wide Mass Spectrometry Center. Microanalyses were performed at the Purdue University Microanalysis Laboratory. Analytical thin-layer chromatography was carried out on Baker-Flex silica gel IB2−F flexible sheets. Compounds were visualized with short wavelength UV light.

(3,4-Dimethoxybenzylidene)-(2,2-dimethoxyethyl)-amine (9). 3,4-Dimethoxybenzaldehyde (**7**, 12.17 g, 0.07323 mol) was dissolved in benzene, (200 mL) and aminoacetaldehydedimethylacetal (**8**, 12.0 mL, 11.7 g, 0.111 mol) was added.

The mixture was stirred at reflux for 4 h using a Dean−Stark trap. The reaction mixture was then concentrated and dissolved in chloroform (250 mL), the solution was washed with water (4 × 150 mL) and brine (150 mL), dried (Na_2SO_4), and concentrated, and the last traces of solvent were removed under vacuum to provide the imine as a light yellow solid (18.55 g, 100%): mp 51−52 °C. ^{1}H NMR (300 MHz, $CDCl_3$) δ 8.09 (s, 1 H), 7.33 (d, J = 1.8 Hz, 1 H), 7.07 (dd, J_1 = 1.8 Hz, J_2 = 8.3 Hz, 1 H), 6.77 (d, J = 8.1, 1 H), 4.57 (t, J = 5.1 Hz, 1 H), 3.83 (s, 3 H), 3.80 (s, 3 H), 3.65 (dd, J_1 = 5.1 Hz, J_2= 1.2 Hz, 2 H), 3.32 (s, 6 H); low resolution ESIMS *m/z* (rel intensity) 254 (MH^+, 66), 222 (100). Anal. ($C_{13}H_{19}NO_4 \cdot 0.1CHCl_3$) C, H, N.

(3,4-Dimethoxybenzyl)-(2,2-dimethoxyethyl)amine (10). The imine **9** (13.90 g, 0.05488 mol) was dissolved in ethanol (50 mL), and $NaBH_4$ (4.20 g, 0.111 mol) was added over 1 h while the reaction mixture was stirred at reflux. The reaction mixture was diluted with water (250 mL). The amine was extracted into chloroform (300 mL) and the extract washed with water (2 × 200 mL) and brine (200 mL), dried (Na_2SO_4), and concentrated to provide a clear colorless oil (12.88 g, 91.7%): bp 148 °C (0.35 mmHg). ^{1}H NMR (300 MHz, $CDCl_3$) δ 6.81 (s, 1 H), 6.78 (d, J = 8.1 Hz, 1 H), 6.74 (d, J = 8.1, 1 H), 4.41 (t, J = 5.4 Hz, 1 H), 3.81 (s, 3 H), 3.79 (s, 3 H), 3.67 (s, 2 H), 3.29 (s, 6 H), 2.67 (d, J = 5.4 Hz, 2 H); low resolution ESIMS *m/z* (rel intensity) 256 (MH^+, 34), 151 (100). Anal. ($C_{13}H_{21}NO_4$) C, H, N.

2,3,8,9-Tetramethoxy-11*H*-indeno[1,2-*c*]isoquinoline Hydrochloride (13). The amine **10** (2.93 g, 0.0115 mol) and veratraldehyde (4.11 g, 0.0247 mol) were mixed with concentrated HCl and stirred at 100 °C for 3 h. The reaction mixture was then cooled and washed with ether (50 mL × 3). Then it was brought to a basic pH with NH_4OH. The mixture was extracted with chloroform (4 × 50 mL), and the solution was washed with water (100 mL), dried (Na_2SO_4), and concentrated. The residue was dissolved in chloroform (200 mL). The mixture was filtered, and HCl (2 M in ether, 40 mL) was added to the filtrate. The precipitate that formed was recrystallyzed from methanol (300 mL) to provide a bright yellow hygroscopic solid (0.5938 g, 14%): mp 254−255 °C. ^{1}H NMR (300 MHz, TFA) δ 9.09 (s, 1 H), 7.77 (s, 1 H), 7.62 (s, 1 H), 7.47 (s, 2 H), 7.40 (s, 1 H), 4.30 (s, 2 H), 4.25 (s, 3 H), 4.18 (s, 3 H), 4.09 (s, 3 H), 4.08 (s, 3 H); low resolution ESIMS *m/z* (rel intensity) 338 (100, MH^+). Anal. ($C_{20}H_{20}NO_4Cl \cdot 1.85H_2O$) C, H, N.

2,3-Dimethoxy-8,9-methylenedioxy-11*H*-indeno[1,2-*c*]-isoquinoline Hydrochloride (14). The amine **10** (3.26 g, 0.0128 mol) was reacted with piperonal (**12**, 4.0 g, 0.0267 mol) following a procedure similar to the one described above for compound **13**. Compound **14** was obtained as a yellow hygroscopic precipitate (2.37 g, 52%): mp 238−240 °C. ^{1}H NMR (300 MHz, D_2O) δ 8.30 (s, 1 H), 6.91 (s, 1 H), 6.69 (s, 1 H), 6.44 (s, 1 H), 6.39 (s, 1 H), 5.94 (s, 2 H), 3.78 (s, 3 H), 3.77 (s, 3 H), 3.00 (s, 2 H); low resolution ESIMS *m/z* (rel intensity) 322 (MH^+, 100). Anal. ($C_{19}H_{16}NO_4Cl \cdot 0.85H_2O$) C, H, N.

(3,4-Methylenedioxybenzylidene)-(2,2-dimethoxyethyl)amine (15). Piperonal (**12**, 15.19 g, 0.1001 mol) was reacted in benzene (200 mL) with aminoacetaldehydedimethylacetal (**8**, 15.0 mL, 14.6 g, 0.139 mol) according to the procedure described for compound **9**. The imine was isolated as a clear colorless oil (23.71 g, 100%): bp 147 °C (0.4 mmHg). ^{1}H NMR (300 MHz, $CDCl_3$) δ 8.13 (s, 1 H), 7.33 (s, 1 H), 7.07 (d, J = 8.10 Hz, 1 H), 6.78 (d, J = 8.10 Hz, 1 H), 5.96 (s, 2 H), 4.62 (t, J = 5.4 Hz, 1 H), 3.70 (d, J = 4.2 Hz, 2 H), 3.37 (s, 6 H); low resolution ESIMS *m/z* (rel intensity) 238 (MH^+, 100), 206 (98). Anal. ($C_{12}H_{15}NO_4$) C, H, N.

(3,4-Methylenedioxybenzyl)-(2,2-dimethoxyethyl)-amine (16). The imine **15** (15.97 g, 0.06731 mol) was dissolved in ethanol (150 mL) and reduced with $NaBH_4$ (4.12 g, 0.109 mol) as described previously for the amine **10**. The amine was obtained as a clear colorless oil (15.82 g, 99%): bp 142−143 °C (0.75 mmHg). ^{1}H NMR (300 MHz, $CDCl_3$) δ 6.79−6.69 (m, 3 H), 5.86 (s, 2 H), 4.41 (t, J = 5.4 Hz, 1 H), 3.64 (s, 2 H), 3.30 (s, 6 H), 2.65 (d, J = 5.4 Hz, 2 H); low resolution ESIMS *m/z* (rel intensity) 240 (MH^+, 100). Anal. ($C_{12}H_{17}NO_4$) C, H, N.

8,9-Dimethoxy-2,3-methylenedioxy-11*H*-indeno[1,2-*c*]-isoquinoline Hydrochloride (18). Compound **18** was obtained from the amine **16** (1.79 g, 7.49 mmol) and veratraldehyde (**11**, 3.04 g, 0.018 mol) following the same method as for **13**. The yellow precipitate that formed (0.7649 g, 29%) was collected by filtration. An analytical sample was prepared by recrystallizing 0.3655 g from methanol (50 mL) to form a hygroscopic solid: mp 257−259 °C. ^{1}H NMR (300 MHz, TFA) δ 8.88 (s, 1 H), 7.69 (s, 1 H), 7.39 (s, 1 H), 7.33 (s, 2 H), 6.21 (s, 2 H), 4.18 (s, 2 H), 4.02 (s, 3 H), 4.01 (s, 3 H); low resolution ESIMS *m/z* (rel intensity) 322 (MH^+, 100); high-resolution ESIMS *m/z* (rel intensity) 322.1084 (MH^+, 100) (calculated mass 322.1079). Anal. ($C_{19}H_{16}NO_4Cl \cdot 0.7H_2O$) C, H, N.

2,3-Methylenedioxy-7,8-methylenedioxy-11*H*-indeno-[1,2-*c*]isoquinoline Hydrochloride (19). The amine **16** (6.22, 0.0224 mol) and piperonal (**12**, 10.10 g, 0.06728 mol) were reacted as described previously for compound **13**, but trifluoroacetic acid was used in place of concentrated hydrochloric acid. The pure base (1.501 g, 22%) was obtained. An analytical sample (0.75 g) was purified further by dissolving the sample in trifluoroacetic acid (50 mL) and adding hydrochloric acid (2 M in diethyl ether, 30 mL). The hydrochloride salt was then washed with ether (200 mL) and recrystallized from methanol (75 mL) to obtain a green-yellow hygroscopic solid: mp 237−239 °C. ^{1}H NMR (300 MHz, TFA) δ 8.74 (s, 1 H), 7.51 (s, 1 H), 7.35 (s, 1 H), 7.31 (s, 1 H), 7.16 (s, 1 H), 6.20 (s, 2 H), 6.05 (s, 2 H), 4.12 (s, 3 H); low resolution ESIMS *m/z* (rel intensity) 306 (MH^+, 100). Anal. ($C_{18}H_{12}NO_4Cl \cdot 0.85H_2O$) C, H, N.

7,8,9-Trimethoxy-2,3-methylenedioxy-11*H*-indeno[1,2-*c*]isoquinoline Hydrochloride (20). The amine **16** (2.28 g, 9.52 mmol) and 3,4,5-trimethoxybenzaldehyde (**17**, 3.77 g, 19.2 mmol) were reacted in trifluoracetic acid (25 mL) with stirring at 100 °C for 3 h. The reaction mixture was cooled and hydrochloric acid (2 M in ether, 10 mL) and ether (200 mL) were added. The precipitate was isolated and dissolved in methanol−water-acetone 1:1:1 (250 mL) and NH_4OH was used to bring the mixture to a basic pH. The mixture was extracted with chloroform (350 mL). The organic layer was washed with brine (200 mL), dried (Na_2SO_4), and concentrated. The residue was dissolved in chloroform (60 mL) and hydrochloric acid (2 M in dry ether, 10 mL) was added. The precipitate was collected and washed with hot methanol (10 mL) and ether 20 (mL) to provide a yellow hygroscopic solid (1.65 g, 45%): mp 257−259 °C. ^{1}H NMR (300 MHz, CD_3OD) δ 9.04 (s, 1 H), 7.63 (s, 1 H), 7.51 (s, 1 H), 7.18 (s, 1 H), 6.32 (s, 2 H), 4.28 (3 H), 4.25 (2 H), 3.98 (3 H), 3.90 (s, 3 H); low resolution ESIMS *m/z* (rel intensity) 352 (MH^+, 100). Anal. ($C_{20}H_{18}NO_5Cl \cdot 1.9H_2O$) C, N, H.

(3,4,5-Trimethoxybenzylidene)-(2,2-dimethoxyethyl)-amine (21). Aminoacetaldehydedimethylacetal (**8**, 20.0 mL, 19.5 g, 0.185 mol) was dissolved in chloroform (80 mL), and $MgSO_4$ (15 g) was added. Then 3,4,5-trimethoxybenzaldehyde (**17**, 10.03 g, 0.05112 mol) was also added, and the mixture was stirred at room temperature for 24 h. The reaction mixture was diluted with chloroform (70 mL), washed with water (4 × 150 mL) and brine (150 mL), dried (Na_2SO_4), and concentrated to provide the pure imine as a light yellow oil (14.47 g, 100%): bp > 180 °C (0.4 mmHg). ^{1}H NMR (300 MHz, $CDCl_3$) δ 8.10 (s, 1 H), 6.91 (s, 2 H), 4.58 (t, J = 5.4 Hz, 1 H), 3.81 (s, 6 H), 3.79 (s, 3 H), 3.69 (d, J_1 = 5.4 Hz, J_2 = 1.2 Hz, 2 H), 3.33 (s, 6 H); low resolution ESIMS *m/z* (rel intensity) 284 (MH^+, 100). Anal. ($C_{14}H_{21}NO_5 \cdot 0.35\ CHCl_3$)

(3,4,5-Trimethoxybenzyl)-(2,2-dimethoxyethyl)-amine (22). The imine **21** (11.59 g, 0.04090 mol) was reduced in ethanol (150 mL) with $NaBH_4$ (2.50 g, 0.0661 mol) following the previous procedure (compound **10**). The amine was isolated as a clear light yellow oil (11.66 g, 100%): bp 175−176 °C (1.4 mmHg). ^{1}H NMR (300 MHz, $CDCl_3$) δ 6.47 (s, 2 H), 4.39 (t, J = 5.4 Hz, 1 H), 3.76 (s, 6 H), 3.73 (s, 3 H), 3.65 (s, 2 H), 3.28 (s, 6 H), 2.65 (d, J = 5.4 Hz, 2 H); low resolution ESIMS *m/z* (rel intensity) 286 (MH^+, 79), 181 (100). Anal. Calcd for $C_{14}H_{23}NO_5$: C, 58.93; H, 8.12; N, 4.91. Found: C, 58.66; H, 8.17; N, 4.63.

2,3,4,7,8-Pentamethoxy-11*H*-indeno[1,2-*c*]isoquinoline Hydrochloride (23). The amine **22** (3.56 g, 0.0125 mol) and veratraldehyde (**11**, 4.00 g, 0.0241 mol) were reacted in concentrated hydrochloric acid (25 mL) as described previously for compound **13**. The product was isolated as a yellow hygroscopic solid (0.75 g, 15%): mp 218−220 °C (dec). ^{1}H NMR (300 MHz, CD_3OD) δ 9.24 (s, 1 H), 7.63 (s, 1 H), 7.57 (s, 1 H), 7.34 (s, 1 H), 4.36 (s, 2 H), 4.16 (s, 3 H), 4.12 (s, 3 H), 4.08 (s, 3 H), 3.95 (s, 3 H), 3.94 (s, 3 H); low resolution ESIMS *m/z* (rel intensity) 368 (MH^+, 100). Anal. ($C_{21}H_{22}NO_5Cl\cdot1.6H_2O$) C, H, N.

2,3,4-Trimethoxy-7,8-methylenedioxy-11*H*-indeno[1,2-*c*]isoquinoline Hydrochloride (24). The amine **22** (2.59 g, 9.08 mmol) and piperonal (**12**, 3.50 g, 0.023 mol) were reacted in concentrated hydrochloric acid as described previously for compound **13**. The product was isolated as a yellow solid (0.62 g, 18%). Reprecipitation of the sample (68.7 mg) from methanol (50 mL) afforded analytically pure material as a hygroscopic solid: mp 230−232 °C (dec). ^{1}H NMR (300 MHz, CD_3OD) δ 9.29 (s, 1 H), 7.62 (s, 1 H), 7.53 (s, 1 H), 7.26 (s, 1 H), 6.11 (s, 2 H), 4.41 (s, 2 H), 4.16 (s, 3 H), 4.11 (s, 3 H), 4.08 (s, 3 H); low resolution ESIMS *m/z* (rel intensity) 352 (MH^+, 100). Anal. ($C_{20}H_{18}NO_5Cl\cdot0.45H_2O$) C, H, N.

2,3,4,7,8,9-Hexamethoxy-11*H*-indeno[1,2-*c*]isoquinoline Hydrochloride (25). The amine **22** (2.62 g, 9.19 mmol) and 3,4,5-trimethoxybenzaldehyde (**17**, 3.70 g, 18.9 mmol) were reacted in concentrated hydrochloric acid as described previously for compound **13**. The product was isolated as a yellow hygroscopic solid (1.612 g, 40%): mp 197−199 °C (dec). ^{1}H NMR (300 MHz, CD_3OD) δ 9.20 (s, 1 H), 7.69 (s, 1 H), 7.22 (s, 1 H), 4.51 (s, 2 H), 4.29 (s, 3 H), 4.17 (s, 3 H), 4.12 (s, 3 H), 4.08 (s, 3 H), 3.99 (s, 3 H), 3.90 (s, 3 H); low resolution ESIMS *m/z* (rel intensity) 398 (MH^+, 100). Anal. ($C_{22}H_{24}NO_6Cl\cdot1.95H_2O$) C, H, N.

(2,5-Dimethoxybenzylidene)-(2,2-dimethoxyethyl)-amine (27). Aminoacetaldehydedimethylacetal (**8**, 20.0 mL, 19.5 g, 0.185 mol) was dissolved in chloroform (100 mL) and $MgSO_4$ (10 g) was added. Then 2,5-dimethoxybenzaldehyde (**26**, 7.00 g, 0.0421 mol) was also added, and the mixture was stirred at room temperature for 24 h. The reaction mixture was diluted with chloroform (100 mL), washed with water (2 × 200 mL) and brine (200 mL), dried (Na_2SO_4), and concentrated to provide the pure imine as a light yellow oil (10.64 g, 100%): bp 151 °C (0.4 mmHg). ^{1}H NMR (300 MHz $CDCl_3$) δ 8.66 (s, 1 H), 7.47 (d, J = 3.0 Hz, 1 H), 6.91 (dd, J_1 = 9.0 Hz, J_2 = 3.0 Hz, 1 H), 6.81 (d, J = 9.0 Hz, 1 H), 4.65 (t, J = 5.1 Hz, 1 H), 3.78 (s, 3 H), 3.77 (s, 3 H), 3.76 (dd, J_1 = 5.4 Hz, J_2 = 1.2 Hz, 2 H), 3.38 (s, 6 H); low resolution ESIMS *m/z* (rel intensity) 254 (MH^+, 100). Anal. ($C_{13}H_{19}NO_4$) C, H, N.

(2,5-Dimethoxybenzyl)-(2,2-dimethoxyethyl)amine (28). The imine **27** (10.64 g, 0.04201 mol) was dissolved in ethanol (100 mL) and reduced with $NaBH_4$ (2.60 g, 0.0687 mol) as described previously for compound **10**. The product was isolated as a clear colorless oil (10.71 g, 100%): bp 155 °C (1.3 mmHg). ^{1}H NMR (300 MHz $CDCl_3$) δ 6.79−6.67 (m, 3 H), 4.43 (t, J = 5.7 Hz, 1 H), 3.72 (s, 3 H), 3.71 (s, 3 H), 3.68 (d, J = 2.7 Hz, 2 H), 3.28 (s, 6 H), 2.7 (d, J = 5.7 Hz, 2 H); low resolution ESIMS *m/z* (rel intensity) 256 (MH^+, 100). Anal. ($C_{13}H_{21}NO_4$) C, H, N.

1,4,7,8-Tetramethoxy-11*H*-indeno[1,2-*c*]isoquinoline Hydrochloride (29). The amine **28** (2.82 g, 11.1 mmol) and veratraldehyde (**11**, 4.00 g, 0.030 mol) were reacted in concentrated hydrochloric acid as described previously for compound **13**. The product was isolated as a yellow-orange hygroscopic solid (1.01 g, 24%): mp 242−244 °C. ^{1}H NMR (300 MHz, TFA) δ 9.52 (s, 1 H), 7.75 (s, 1 H), 7.43 (d, J = 7.8 Hz, 1 H), 7.38 (s, 1 H), 7.08 (d, J = 8.7 Hz, 1 H), 4.56 (s, 2 H), 4.10 (s, 3 H), 4.09 (s, 3 H), 4.04 (s, 6 H). Anal. ($C_{20}H_{20}NO_4Cl\cdot1.7H_2O$) C, H, N.

1,4-Dimethoxy-7,8-methylenedioxy-11*H*-indeno[1,2-*c*]-isoquinoline Hydrochloride (30). The amine **28** (2.22 g, 8.69 mmol) and piperonal (**12**, 3.96 g, 0.0264 mol) were reacted in concentrated hydrochloric acid as described previously for compound **13**. The product was isolated as an orange hygroscopic solid (1.6081 g, 52%): mp 245−247 °C (dec). ^{1}H NMR (300 MHz, CD_3OD) δ 9.50 (s, 1 H), 7.56 (s, 1 H), 7.48 (d, J = 8.7 Hz, 1 H), 7.28 (s, 1 H), 7.17 (d, J = 8.7 Hz, 1 H), 6.13 (s, 2 H), 4.47 (s, 2 H), 4.10 (s, 6 H); low resolution ESIMS *m/z* (rel intensity) 322 (MH^+, 100). Anal. ($C_{19}H_{16}NO_4Cl\cdot0.5H_2O$) C, H, N.

(2,3,4-Trimethoxybenzylidene)-(2,2-dimethoxyethyl)-amine (32). 2,3,4-Trimethoxybenzaldehyde (**31**, 11.48 g, 0.05851 mol) was dissolved in benzene (200 mL) and aminoacetaldehydedimethylacetal (**8**, 10.0 mL, 9.75 g, 0.0927 mol) was added. The same procedure was applied as for **9**. The product was isolated as a clear light yellow oil (16.58 g, 100%): bp 153−155 °C (0.45 mmHg). ^{1}H NMR (300 MHz $CDCl_3$) 8.49 (s, 1 H), 7.64 (d, J = 8.7 Hz, 1 H), 6.65 (d, J = 8.7 Hz, 1 H), 4.61 (t, J = 5.4 Hz, 1 H), 3.88 (s, 3 H), 3.84 (s, 3 H), 3.82 (s, 3 H), 3.71 (d, J = 5.4 Hz, 2 H), 3.36 (s, 6 H); low resolution ESIMS *m/z* (rel intensity) 284 (MH^+, 100), 252 (45). Anal. ($C_{14}H_{21}NO_5$)

(2,3,4-Trimethoxybenzyl)-(2,2-dimethoxyethyl)amine (33). The imine **32** (14.28 g, 0.05040 mol) was dissolved in ethanol (100 mL) and reacted with $NaBH_4$ (3.00 g, 0.0793 mol) as described previously for compound **10**. A colorless oil (14.38 g, 100%) was obtained. ^{1}H NMR (300 MHz, $CDCl_3$) δ 6.89 (d, J = 8.4 Hz, 1 H), 6.57 (d, J = 8.4 Hz, 1 H), 4.45 (t, J = 5.4 Hz, 1 H), 3.87 (s, 3 H), 3.82 (s, 3 H), 3.80 (s, 2 H), 3.70 (s, 3 H), 3.31 (s, 6 H), 2.68 (d, J = 5.4 Hz, 2 H); low resolution ESIMS *m/z* (rel intensity) 286 (MH^+, 100), 181 (69). Anal. ($C_{14}H_{23}NO_5$) C, H, N

1,2,3,7,8-Pentamethoxy-11*H*-indeno[1,2-*c*]isoquinoline Hydrochloride (34). The amine **33** (2.67, 9.36 mmol) and 3,4-dimethoxybenzaldehyde (**11**, 3.23 g, 0.195 mol) were reacted in concentrated hydrochloric acid as described previously for compound **13**. The product was isolated as a yellow hygroscopic solid (135.5 mg, 5%): mp 201−203 °C. ^{1}H NMR (300 MHz, CD_3OD) δ 9.26 (s, 1 H), 7.67 (s, 1 H), 7.39 (s, 1 H), 7.27 (s, 1 H), 4.26 (s, 3 H), 4.22 (s, 2 H), 4.17 (s, 3 H), 3.98 (s, 3 H), 3.97 (s, 3 H), 3.96 (s, 3 H); low resolution ESIMS *m/z* (rel intensity) 368 (MH^+, 100). Anal. ($C_{21}H_{22}NO_5Cl\cdot1.8H_2O$) C, H, N.

1,2,3-Trimethoxy-7,8-methylenedioxy-11*H*-indeno[1,2-*c*]isoquinoline Hydrochloride (35). The amine **33** (3.03, 10.7 mmol) and piperonal (**12**, 3.96 g, 0.0264 mol) were were reacted in concentrated hydrochloric acid as described previously for compound **13**. The product was isolated as an yellow hygroscopic solid (0.353 g, 8.5%): mp 206−207 °C. ^{1}H NMR (300 MHz, CD_3OD) δ 9.26 (s, 1 H), 7.52 (s, 1 H), 7.27 (s, 2 H), 6.11 (s, 2 H), 4.25 (s, 3 H), 4.21 (s, 2 H), 4.16 (s, 3 H), 3.97 (s, 3 H); low resolution ESIMS *m/z* (rel intensity) 352 (MH^+, 100). Anal. ($C_{20}H_{18}NO_5Cl\cdot0.15H_2O$) C, H, N.

1,2,3,7,8,9-Hexamethoxy-11*H*-indeno[1,2-*c*]isoquinoline Hydrochloride (36). The amine **33** (3.23, 11.4 mmol) and 3,4,5-trimethoxybenzaldehyde (**17**, 4.04 g, 0.0206 mol) were reacted in concentrated hydrochloric acid as described previously for compound **13**. The product was isolated as a hygroscopic yellow solid (0.5203 g, 10.5%): mp 196−198 °C. ^{1}H NMR (300 MHz, CD_3OD) δ 9.12 (s, 1 H), 7.27 (s, 1 H), 7.20 (s, 1 H), 4.30−4.26 (8 H), 4.18 (s, 2 H), 3.99 (s, 3 H), 3.98 (s, 3 H), 3.90 (s, 3 H); low resolution ESIMS *m/z* (rel intensity) 398 (MH^+, 100). Anal. ($C_{22}H_{24}NO_6Cl\cdot1.4H_2O$) C, H, N.

Topoisomerase I-Mediated DNA Cleavage Reactions Using 3′-End-Labeled 161 BP Plasmid DNA. The assays were conducted as previously described.[5] Briefly, the 161 bp fragment obtained after the cleavage of pBluescript SK(−) phagemid DNA (Stratagene, La Jolla. CA) with restriction endonuclease Pvu II and Hind III (New England Biolabs, Beverly, MA) was endlabeled at the Hind III site by fill-in reaction with [α-^{32}P]-dCTP and dATP, dGTP and dTTP. The labeled DNA fragment was incubated with top1 for 30 min at 30 °C in the presence of the synthetic compound to be tested. After precipitation with ethanol, the samples in loading buffer were separated on a denaturing gel (16% polyacrylamide, 7 M urea) at 51 °C. The gel was visualized by using Phosphoimager.

DNA Cleavage Semiquantitative Analysis. One of the most abundant cleavage products, specifically the sequence

previously labeled 44,[8] was chosen for semiquantitation using ImageQuant TL v2003.3. The rubberband baseline correction was applied with band detection sensitivity set at 90. In the case of each norindenoisoquinoline the absolute density value for the band corresponding to the above product was compared to the value for the standard substance, NSC 314622. The ratio of the norindenoisoquinoline band density to the NSC 314622 band was multiplied by 100 to obtain percentages. Assignments were performed as follows: 0−25% 0; 25−75% +; 75−175% ++; 175−325% +++; camptothecin ++++.

Molecular Modeling of the Crystal Structure. The diagram of the crystal structure (Figure 3) was prepared starting from the pdb file and the Sybyl 6.9 software package from Tripos. Missing bonds were added in the phosphodiester backbone, in T10 as well as the bond to the sulfur atom of the DNA oligonucleotide. The atom types of the DNA strands were corrected according to Sybyl types. The atom types for the end groups were also corrected according to Sybyl types and assigned as charged residues. The software correctly assigned atom types in the protein structure except for the amino terminus. No missing bonds were identified in the enzyme.

Crystallization and Structure Determination of the Ternary Complex. A 70 kDa construct of human topoisomerase I (topo70), residues Lys175 to Phe765, was expressed and purified from baculovirus-insect cells (SF9) as described previously.[34] The covalent complex of topo70−DNA was prepared using a 5′ bridging phosphorothiolate duplex oligonucleotide previously described.[35] The oligonucleotide sequence of the cleavable strand of the duplex oligomer was 5′-AAAAAGACTTsCGAAAAATTTTT-3′ where 's' represents the 5′ bridging phosphorothiolate of the cleaved strand. Ternary complex crystals were grown by sitting drop vapor diffusion by preparing drops containing 2.0 μL of precipitant, 1.5 μL of 50 μM duplex DNA, 0.5 μL of compound, and 1.5 μL of of 4.2 mg/mL protein. Precipitant was 10−12% PEG 8000, 100mM MES pH 6.4, 200 mM lithium sulfate. Compound **14** was dissolved in water and diluted with preciptant to final concentrations of 1, 2, 5, and 10 mM for crystallization trials. Crystals were cryoprotected for data collection by passing them through precipitant plus 30% v/v PEG 400. Data were collected at 100 K at beamline 5.0.3, Advanced Light Source, Lawrence Berkely National Laboratory. Crystals were isomorphous with previous topo70−DNA complex crystal structures[33] and the protein model was positioned by rigid body refinement. Refinements were conducted using CNX[36] and iterative model adjustments with XtalView.[37] DNA's were placed into the |Fo|-|Fc| electron density and refined. Compound **14** model was then placed into the |Fo|-|Fc| electron density using XtalView and refined. Data and refinement statistics are presented in Table 2. The highest resolution of the X-ray data obtained was 3.1 Å and did not allow the placement of water molecules.

Computer Modeling. Norindenoisoquinoline **25** was minimized prior to its inclusion in the ternary complex using the MMFF94s force field, MMFF94 charges, and the conjugate gradient method, with no initial optimization, to a gradient of less than 0.05 kcal/mol. Then norindenoisoquinoline **25** was placed in the ternary complex of the crystal structure in the same orientation as norindenoisoquinoline **14**, and the ligand **14** was deleted. The resulting complex was minimized in two different manners. First it was minimized as a subset using the Powell method, MMFF94s force field and MMFF94 charges to a gradient of 0.5 kcal/mol or less. The protein backbone atoms were included into an aggregate and their positions remained fixed. The atoms not included in the aggregate in a sphere of 6 Å around the ligand were allowed to move during energy minimization; atoms included in a shell stretching from 6 to 12 Å were also allowed to move yet to a lesser extent (radius of hot region 6 Å, radius of interesting region 12 Å).

The result indicated that the adjacent DNA base, thiocytidine, was flipped in part to avoid steric interference with the methoxy substituents. Steric conflicts still appeared to persist between Arg364 and the methoxy group in position 7 and between the ligand methoxy in position 3 and the deoxyribose (C1′, C5′) of thiocytidine 11 (TCP 11). Unfavorable contacts were also detected between the sugar−phosphate backbone of the nonscissile DNA strand and the methoxy group in position 8. Stacking interactions appeared to be decreased as in the resulting complex there was little contact between the norindenoisoquinoline **25** and the neighboring pyrimidine bases. These are regions where in the crystal structure there is good overlap and favorable van der Waals interaction due to dispersion forces. During energy minimization the ligand moved about 1 Å away from Arg364 and there is no hydrogen bonding interaction between the norindenoisoquinoline **25** and Arg364.

The second minimization was carried out in the same way except an aggregate was used that included both the protein backbone atoms and all the DNA substructures. In the resulting complex, since the DNA bases had been frozen, the neighboring bases could not move away to avoid steric clashes and additional unfavorable contacts were detected between the norindenoisoquinoline **25** (the methoxy substituents in positions 2 and 7) and the neighboring thymine (T10), adenine (ADE113), and guanine (GUA112).

Table 2. Refinement Statistics[b]

inhibitor bound	AI-III-52
PDBID	1TL8
resolution (Å)	50−3.1 (3.21−3.10)
no. reflections	16738 (1581)
R_{sym}[a]	10.0 (52.2)
completeness	97.8 (93.1)
$I/\sigma I$	13.7 (2.3)
space group	P21
a (Å)	56.949
b (Å)	114.140
c (Å)	73.499
β	94.18
reflections used in RFREE	5%, 808
no. of protein atoms	4703
no. of DNA atoms	892
no. of inhibitor atoms	24
no. of solvent atoms	0
R_{factor}	22.9 (33.2)
R_{free}	30.5 (39.5)
rms deviations from ideal stereochemistry	
bond lengths (Å)	0.017
bond angles (deg)	1.9
impropers (deg)	3.94
dihedrals (deg)	23.8
mean B_{factor}, all atoms (Å^3)	60.4

[a] $R_{sym} = \Sigma |I_i - I_m| / \Sigma I_m$ where I_i is the intensity of the measured reflection and I_m is the mean intensity of all symmetry related reflections. [b] Numbers in parentheses represent final shell of data.

Acknowledgment. This work was made possible by the National Institutes of Health (NIH) through support of this work with Research Grant UO1 CA89566. The in vitro and in vivo testing was conducted through the Developmental Therapeutics Program, DCTD, NCI under Contract NO1-CO-56000. The Advanced Light Source is supported by the Director, Office of Science, Office of Basic Energy Sciences, Materials Sciences Division, of the U.S. Department of Energy under Contract No. DE-AC03-76SF00098 at Lawrence Berkeley National Laboratory. We are grateful to Prof. V. Jo Davisson for allowing the use of the densitometer and ImageQuant TL v2003.3 software. This research was conducted in a facility constructed with support from Research Facilities Improvement Program Grant Number C06-14499 from the National Center for Research Resources of the National Institutes of Health.

Supporting Information Available: Elemental analysis data. This material is available free of charge via the Internet at http://pubs.acs.org.

References

(1) Kohlhagen, G.; Paull, K.; Cushman, M.; Nagafuji, P.; Pommier, Y. Protein-Linked DNA Strand Breaks Induced by NSC 314622, a Novel Noncamptothecin Topoisomerase I Poison. *Mol. Pharmacol.* **1998**, 54, 50−58.

(2) Li, T. K.; Liu, L. F. Tumor Cell Death Induced by Topoisomerase-Targeting Drugs. *Annu. Rev.* Pharmacol. Toxicol. **2001**, *41*, 53−77.

(3) Burke, T. G.; Mi, Z. H. The Structural Basis of Camptothecin Interactions with Human Serum-Albumin − Impact on Drug Stability. *J. Med. Chem.* **1994**, *37*, 40−46.

(4) Cushman, M.; Jayaraman, M.; Vroman, J. A.; Fukunaga, A. K.; Fox, B. M.; Kohlhagen, G.; Strumberg, D.; Pommier, Y. Synthesis of New Indeno[1,2-*c*]isoquinolines: Cytotoxic Non-Camptothecin Topoisomerase I Inhibitors. *J. Med. Chem.* **2000**, *43*, 3688−3698.

(5) Strumberg, D.; Pommier, Y.; Paull, K.; Jayaraman, M.; Nagafuji, P.; Cushman, M. Synthesis of Cytotoxic Indenoisoquinoline Topoisomerase I Poisons. *J. Med. Chem.* **1999**, *42*, 446−457.

(6) Jayaraman, M.; Fox, B. M.; Hollingshead, M.; Kohlhagen, G.; Pommier, Y.; Cushman, M. Synthesis of New Dihydroindeno-[1,2-*c*]isoquinoline and Indenoisoquinolinium Chloride Topoisomerase I Inhibitors Having High in Vivo Anticancer Activity in the Hollow Fiber Animal Model. *J. Med. Chem.* **2002**, *45*, 242−249.

(7) Pommier, Y.; Pourquier, P.; Fan, Y.; Strumberg, D. Mechanism of Action of Eukaryotic DNA Topoisomerases and Drugs Targeted to the Enzyme. *Biochim. Biophys. Acta* **1998**, *1400*, 83−105.

(8) Antony, S.; Jayaraman, M.; Laco, G.; Kohlhagen, G.; Kohn, K. W.; Cushman, M.; Pommier, Y. Differential Induction of Topoisomerase I-DNA Cleavage Complexes by the Indenoisoquinoline MJ-III-65 (NSC 706744) and Camptothecin: Base Sequence Analysis and Activity against Camptothecin-Resistant Topoisomerase I. *Cancer Res.* **2003**, *63*, 7428−7435.

(9) Staker, B. L.; Feese, M. D.; Cushman, M.; Pommier, Y.; Zembower, D.; Stewart, L.; Burgin, A. B. Structures of Three Classes of Anticancer Agents bound to the Human Topoisomerase I-DNA Covalent Complex. *J. Med. Chem.* **2005**, *48*, 2336−2345.

(10) Dyke, S. F.; Sainsbury, M.; Brown, D. W.; Palfreyman, M. N.; Wiggins, D. W. 1,2-Dihydroisoquinolines-XVI Indeno[1, 2-*c*]-isoquinoline Derivatives. *Tetrahedron* **1971**, *27*, 281−289.

(11) Gensler, W. J.; Shamasundar, K. T.; Marburg, S. Synthesis of 11*H*-Indenoisoquinolines Related to Cherlerythrine. *J. Org. Chem.* **1968**, *33*, 2861−2868.

(12) Brown, D. W.; Dyke, S. F.; Sainsbury, M. 1,2-Dihydroisoquinolines X. The Cyclization of Benzaldehyde Dialkylacetals. *Tetrahedron* **1969**, *30*, 101−117.

(13) Bobbitt, J. M.; Winter, D. P.; Kiely, J. M. Synthesis of Isoquinolines. IV.[1] 4-Benzylisoquinolines. *J. Org. Chem.* **1965**, *30*, 2459−2460.

(14) Bobbitt, J. M.; Bourque, A. J. Synthesis of Heterocycles Using Aminoacetals. *Heterocycles* **1987**, *25*, 601−616.

(15) Gee, K. R.; Barmettler, P.; Rhodes, M. R.; McBurney, R. N.; Reddy, N. L.; Hu, L. Y.; Cotter, R. E.; Hamilton, P. N.; Weber, E.; Keana, J. F. 10.5-(Iminomethano)-10,11-dihydro-5*H*-dibenzo-[*a*,*d*]cycloheptene and Derivatives. Potent PCP Receptor Ligands. *J. Med. Chem.* **1993**, *36*, 1938−1946.

(16) Suzuki, T.; Takamoto, M.; Okamoto, T.; Takayama, H. Acid-Catalyzed Double-Cyclization Reactions of *N,N*-Dibenzylaminoacetaldehyde Dialkyl Acetals and Related Compounds: General Synthesis of 7,12-Dihydro-5*H*-6,12-Methanobenz[*c*,*f*]azocines and Related Compounds. *Chem. Pharm. Bull.* **1986**, *34*, 1888−1900.

(17) Gensler, W. J. The Synthesis of Isoquinolines by the Pomeranz-Fritsch Reaction. *Org. React.* **1951**, *6*, 191−206.

(18) Bobbitt, J. M. Chemistry of 4-Hydroxy- and 4-Keto-1,2,3,4-tetrahydroisoquinolines. *Adv. Heterocycl. Chem*. **1973**, *15*, 99−126.

(19) Birch, A. J.; Jackson, A. H.; Shannon, P. V. R. New Modification of the Pomeranz-Fritsch Isoquinoline Synthesis. *J. Chem. Soc, Perkin Trans. 1* **1974**, 2185−2194.

(20) Bevis, M. J.; Forbes, E. J.; Uff, B. C. The Use of Phoyphosphoric Acid in the Pomeranz-Fritsch Synthesis of Isoquinolines. *Tetrahedron* **2001**, *25*, 1585−1589.

(21) Kakefuda, A.; Watanabe, T.; Takahashi, T.; Sakamoto, S.; Tsukamoto, S. I. An Efficient Synthesis of (±)-6,7-Dimethoxy-1-oxo-2-(3-pyridiyl)-1,2,3,4-tetrahydroisoquinoline. *Synth. Commun.* **2001**, 401−408.

(22) Cushman, M.; Cheng, L. Stereoselective Oxidation by Thionyl Chloride Leading to the Indeno[1,2-*c*]isoquinoline System. *J. Org. Chem.* **1978**, *43*, 3781−3783.

(23) Simig, G. Synthesis of 1,2-Dihydroisoquinoline-3-carbaldehydes. *J. Chem. Res., Synop.* **1992**, 36−37.

(24) Euerby, M. R.; Waigh, R. D. Regioselectivity in the Synthesis of Isoquinolines with Methoxy Activating Groups. *J. Chem. Res., Synop.* **1987**, 36−37.

(25) Bobbitt, J. M.; Kiely, J. M.; Khanna, K. L.; Ebermann, R. Synthesis of Isoquinolines. 111. A New Synthesis of 1,2,3,4-Tetrahydroisoquinolines. *J. Org. Chem.* **1965**, *1965*, 2247−2250.

(26) Paul, R.; Coppola, J. A.; Cohen, E. 1-Phenyl-1,2,3,4-tetrahydroisoquinolines. A New Series of Nonsteroidal Female Antifertility Agents. *J. Med. Chem.* **1972**, *15*, 720−726.

(27) Schlosser, M.; Simig, G.; Geneste, H. Three Complementary Methods Offering Access to 5-Substituted 1,2,3,4-Tetrahydroisoquinolines. *Tetrahedron* **1998**, *54*, 9023−9032.

(28) Bobbitt, J. M.; Sih, J. C. Synthesis of Isoquinolines. VII. 4-Hydroxy-1,2,3,4-tetrahydroisoquinolines.[1] *J. Org. Chem.* **1968**, *33*, 856−858.

(29) Brown, D. W.; Dyke, S. F.; Palfreyman, M. N.; Sainsbury, M. The Influence of Acids on 4-Benzyl-1,2-dihydroisoquinoline Derivatives. *Tetrahedron Lett.* **1968**, *54*, 5615−5618.

(30) Dyke, S. F.; Sainsbury, M.; Moon, B. J. 1,2-Dihydroisoquinolines-VII New Synthesis of Avicine and Nitidine Derivatives. *Tetrahedron* **1968**, *24*, 1467−1474.

(31) Pommier, Y.; Fesen, M. R.; Goldwasser, F. Topoisomerase II Inhibitors: the Epipodophyllotoxins, *m*-AMSA, and the Ellipticine Derivatives. *Cancer Chemotherapy and Biotherapy: Principles and Practice*; Lippincott-Raven: Philadelphia, 1996; pp 435−461.

(32) Nagarajan, M.; Morrell, A.; Fort, B. C.; Meckley, M. R.; Antony, S.; Kohlhagen, G.; Pommier, Y.; Cushman, M. Synthesis and Anticancer Activity of Simplified Indenoisoquinoline Topoisomerase I Inhibitors Lacking Substituents on the Aromatic Rings. *J. Med. Chem.* **2004**, *47*, 5651−5661.

(33) Staker, B. L.; Hjerrild, K.; Feese, M. D.; Behnke, C. A.; Burgin Jr., A. B.; Stewart, L. The Mechanism of Topoisomerase I Poisoning by a Camptothecin Analog. *Proc. Natl. Acad. Sci. U.S.A.* **2002**, *99*, 15387−15392.

(34) Stewart, L.; Ireton, G. C.; Parker, L. H.; Madden, K. R.; Champoux, J. J. Biochemical and Biophysical Analysis of Recombinant Forms of Human Topoisomerase I. *J. Biol. Chem.* **1996**, *271*, 7593−7601.

(35) Burgin Jr., A. B.; Huitzenga, B. N.; Nash, H. A. A Novel Suicide Substrate for DNA Topoisomerases and Site-Specific Recombinases. *Nucleic Acids Res.* **1995**, *23*, 2973−2979.

(36) Brünger, A. T.; Adams, P. D.; Clore, G. M.; DeLano, W. L.; Gros, P.; Grosse-Kunstleve, R. W.; Jiang, J.-S.; Kuszewski, J.; Nilges, M.; Pannu, N. S.; Read, R. J.; Rice, L. M.; Simonson, T.; Warren, G. L. Crystallography and NMR System: A New Software Suite for Macromolecular Structure Determination. *Acta Crystallogr.* **1998**, *D54*, 905−921.

(37) McRee, D. E. XtalView/Xfit − A Versatile Program for Manipulating Atomic Coordinates and Electron Density. *J. Struct. Biol.* **1999**, *125*, 156−165.

JM050076B